

RESEARCH ARTICLE

Open Access



Vertical profiles of arsenic and arsenic species transformations in deep-sea sediment, Nankai Trough, offshore Japan

Harue Masuda^{1*} , Haruka Yoshinishi¹, Shigeshi Fuchida^{1,2}, Tomohiro Toki³ and Emilie Even¹

Abstract

Concentrations of arsenic (As) and its chemical forms were determined on deep-sea sediments drilled at three sites of Nankai Trough, off the Kii Peninsula, Japan. Those sediments were analyzed to document the behavior of As in relation to methane hydrate formation and the deep biosphere.

The analytical results showed the total As concentration of interstitial water (IW) and squeezed cake (SC) ranged from 0.9 to 380 ppb and from 3 to 14 ppm (average, 6.4 ppm), respectively. The sediments from Site C0002, of which sediment column was the longest down to 2200 m below the seafloor (mbsf) among the studied three drilling sites, were analyzed for the host phase transformation of As. The total concentration of As of IW and SC from 200 to 500 mbsf, where methane hydrate zone was included, was higher than those from the uppermost 200 m. Concentration of As was ultimately controlled by pH. Also, organoarsenicals, such as methylarsonic acid (MMA) and arsenobetaine (AsB), were detected in the sediment column, implying that these organoarsenicals appeared in relation to the in situ microbial activities. These observations suggest that As becomes mobilized directly or indirectly as a result of microbial activity in deep-sea sediments.

Keywords: Nankai Trough, Deep biosphere, Organoarsenical, Convergent margin

Introduction

Distribution and behavior of arsenic (As), one of the most common toxic elements, in the hydrosphere and subareal and under-water shallow sediments have been well documented as a part of geologic cycle of arsenic in the Earth's surface and crust (e.g., Masuda 2018, and references therein). The As is generally present in clean, open-ocean water at an average concentration of 1.5 µg/L (e.g., Andreae 1979). Marine organisms, particularly photosynthetic organisms, take up As from seawater and accumulate it in their bodies, where metabolic reactions result in As species transformations. Biogeochemical processes affecting As in ocean water have been well documented (e.g., Neff 2002, and references therein); in marine organisms, As is present as both inorganic species such as arsenate (As^V) and arsenite (As^{III}) (e.g., Sanders 1979; Raab et al. 2005; Duncan et al. 2015) and organic species,

such as arsenosugars in marine algae (e.g., Morita and Shibata 1990; Edmonds et al. 1997; Raab et al. 2005) and arsenobetaine in marine animals (e.g., Edmonds et al. 1977; Duncan et al. 2015).

In general, the dominant As phases in sediments are the inorganic species: that is, arsenite in reducing environments and arsenate in oxidizing environments (Neff 2002). Unpolluted nearshore marine and estuarine sediments usually contain from 5 to 15 µg/g As, but deep-sea sediments occasionally contain much higher concentrations, probably owing to precipitation from submarine hydrothermal solutions. Neff (2002) documented As phase changes in marine sediments due to microbial decomposition and synthesis of organoarsenicals and reported that sulfides such as realgar (As₄S) and pyrite (FeS₂), in which As was included as an impurity element, and oxides such as arsenolite (As₂O₃) are the main final inorganic products fixed in the sediments.

In coastal areas, As in sediments and interstitial water has been studied mainly in relation to biotoxicity. In deep-sea environments, although As has been documented

* Correspondence: harue@sci.osaka-cu.ac.jp

¹Department of Biology and Geosciences, Graduate School of Science, Osaka City University, 3-3-138 Sugimoto, Sumiyoshi-ku, Osaka 558-8585, Japan
Full list of author information is available at the end of the article

in seafloor surface sediments (e.g., Francesconi and Edmonds 1996) and in hydrothermal sediments (e.g., Handley and Lloyd, 2013), vertical profiles of As in deep-sea sediments have not been systematically studied. In this study, we first traced concentrations and chemical forms of As in deep-sea sediments from the seafloor surface, through a methane hydrate layer, and down to 2200 mbsf. Then, we examined the sources of As and effect of microbial activity on its behavior in deep-sea sediments.

Samples and analytical methods

Drilling sites and studied cores

The sediment cores used in this study were collected from three different drilling sites around the Nankai Trough (Sites C0002, C0021, and C0022) by D/V *Chikyu* during various Integrated Ocean Drilling Program (IODP) expeditions (Fig. 1).

The longest core was from Site C0002 in the Kumano Forearc Basin. The sediments at this site were lithologically categorized into five units (Moore et al. 2013; Expedition 348 Scientists and Scientific Participants 2014): in descending order, Unit I (shallower than 126 mbsf) consists of hemipelagic mud with fine sand, silt, and volcanic ash deposited since 1 Ma; Unit II (126–826 mbsf), which has a similar lithology to Unit I but consists of more consolidated sediments, was deposited between 1.67 and 1 Ma; Unit III (826–1025.5 mbsf) is composed of slope sediments deposited during a period of slow sedimentation from 3.65 to 1.67 Ma; Unit IV (1025.5–1740.5 mbsf) is composed of accretionary prism sediments older than 5.6 Ma (Ashi et al. 2008); and Unit V (1740.5–2220 mbsf) consists of accretionary prism sediments older than those of Unit IV. Cuttings and logging data suggest that Unit V is somewhat sandy with many conductive fractures. A bottom-simulating reflector (Moore et al. 2009; Strasser et al. 2014) and onboard infrared-camera observations of low-temperature anomalies at 369, 388, and 392 mbsf in the recovered sediment cores (Moore et al. 2013) confirm the presence of methane hydrate at 200 to 400 mbsf in Unit II. Reduced chlorinity in interstitial water (IW) from 200 to 400 mbsf also supports the presence of the methane hydrate in this depth interval (Fig. 2, Moore et al. 2013).

Site C0022 is located on the toe of the forearc slope of the Nankai Trough (Fig. 1). On the basis of their overall lithology, the cored sediments down to 415.9 mbsf were classified into a single unit, although two subunits were identified in logging data during drilling (Moore et al. 2013): Subunit II-a (0–383.5 mbsf) is composed dominantly of silty clay with variable amounts of calcareous nanofossils, foraminifers, siliceous biogenic debris, and volcanic ash; Subunit II-b (383.5–415.9 mbsf) consists of a series of mud-encrusted gravels interbedded with thin sand, clayey silt, and silty clay layers in its upper part and

with mainly silty clay layers in its lower part. Several shear zones and minor faults indicate the presence of a splay fault in the interval from 80 to 140 mbsf. Below this fracture zone, chlorinity of the IW was higher than that of ambient seawater (Fig. 3c), presumably because of upwelling of deep-seated water along the fault (Moore et al. 2013).

Site C0021, located on the basin slope seaward of the splay fault, is composed of dominantly silty clay sediments that were relocated by a submarine landslide (Moore et al. 2013). The chlorinity of the IW, which was the same as that of seawater, was uniform from the seafloor to 200 mbsf (Fig. 3g), probably as a result of homogenization of the collapsed sediments.

Most core samples used for our As analyses were collected by IODP Expedition 338 (October 2012 to January 2013) from Hole C0021B (drilled interval 0–204 mbsf), Hole C0022B (drilled interval 0–204 mbsf), Holes C0002K, L (200–505 mbsf), and holes C0002J and H (902–940 and 1100.5–1120 mbsf, respectively) (Moore et al. 2013). Both stored and newly recovered cores from Site C0002 were analyzed to document As behavior from the seafloor to as deep as possible in the ocean bottom sediments. Sediment samples from 0 to 204 mbsf and 475–1057 mbsf in Holes C0002D and B, respectively, were collected by Expedition 315 (November–December 2007) (Ashi et al. 2008), and those from 2110 to 2220 mbsf in Holes C0002P were collected by Expedition 348 (September 2013 to January 2014) (Expedition 348 Scientists and Scientific Participants 2014).

Analytical methods

In order to examine As in coexisting water and solids, we analyzed As in both IW and the squeezed cake (SC, residual sediment after extraction of IW). IW was extracted from the sediment cores on board with a Manheim-type titanium squeezer (Manheim 1966), filtered through a polytetrafluoroethylene (PTFE) membrane filter (0.45 μm mesh), preserved with HCl in a plastic vial (Nalgene), and stored at room temperature. The SC was stored onboard at -20°C during the cruises. Then, in the shore-based laboratory, the SC was freeze-dried and powdered manually for the analyses. In our analyses, we used stored IW from shallow sediments above 200 mbsf in Site C0002 that had previously been used for onboard analysis of alkalinity. Among the samples taken during Expedition 348, we analyzed only the SC, because these core samples rarely contained an extractable amount of IW.

We determined total As concentrations in the bulk sediment (i.e., SC) and dissolved in the IW, As species extracted from the sediments by a sequential chemical extraction method, and As species in the sediments separated by high-performance liquid chromatography (HPLC) as described below.

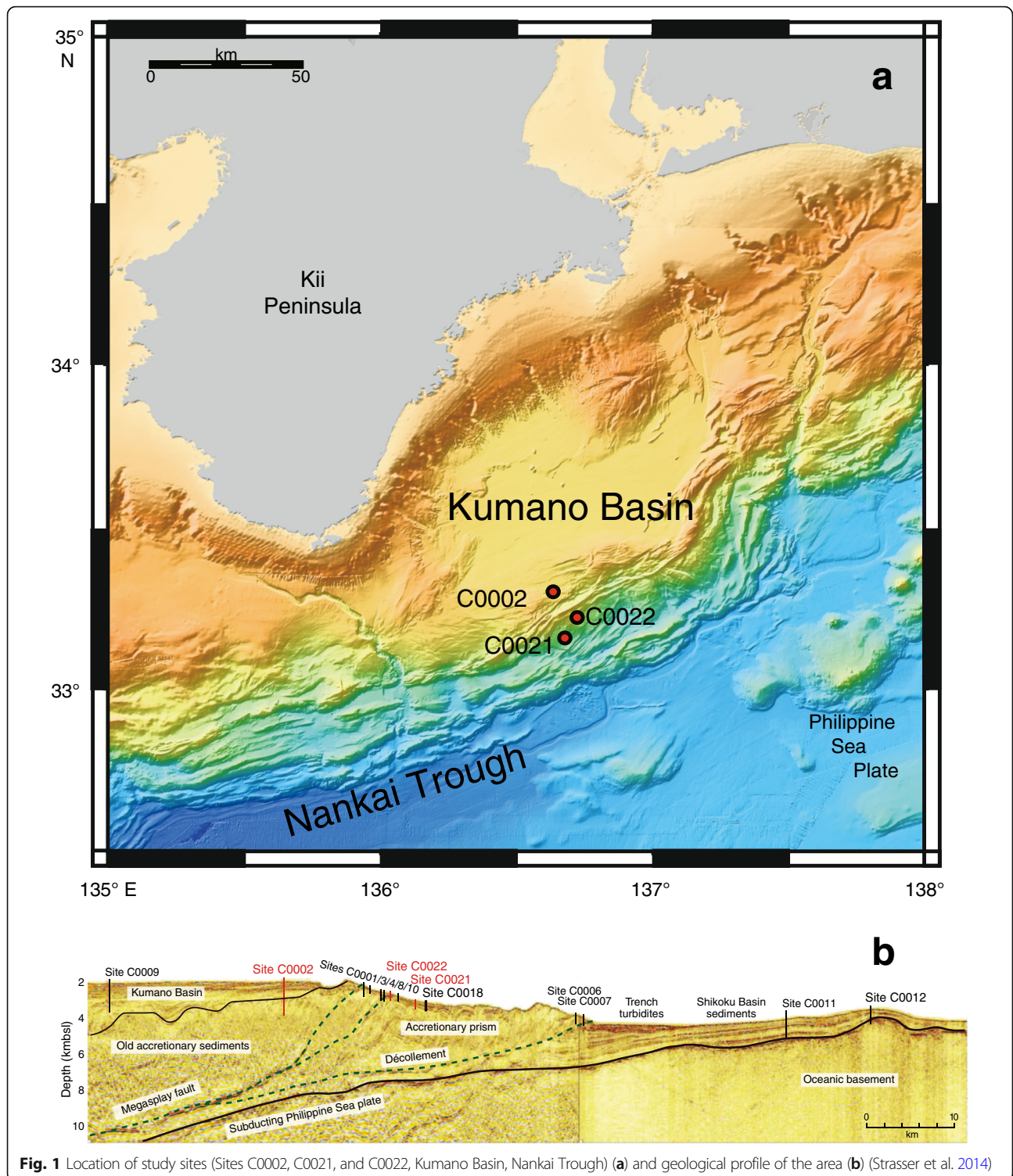
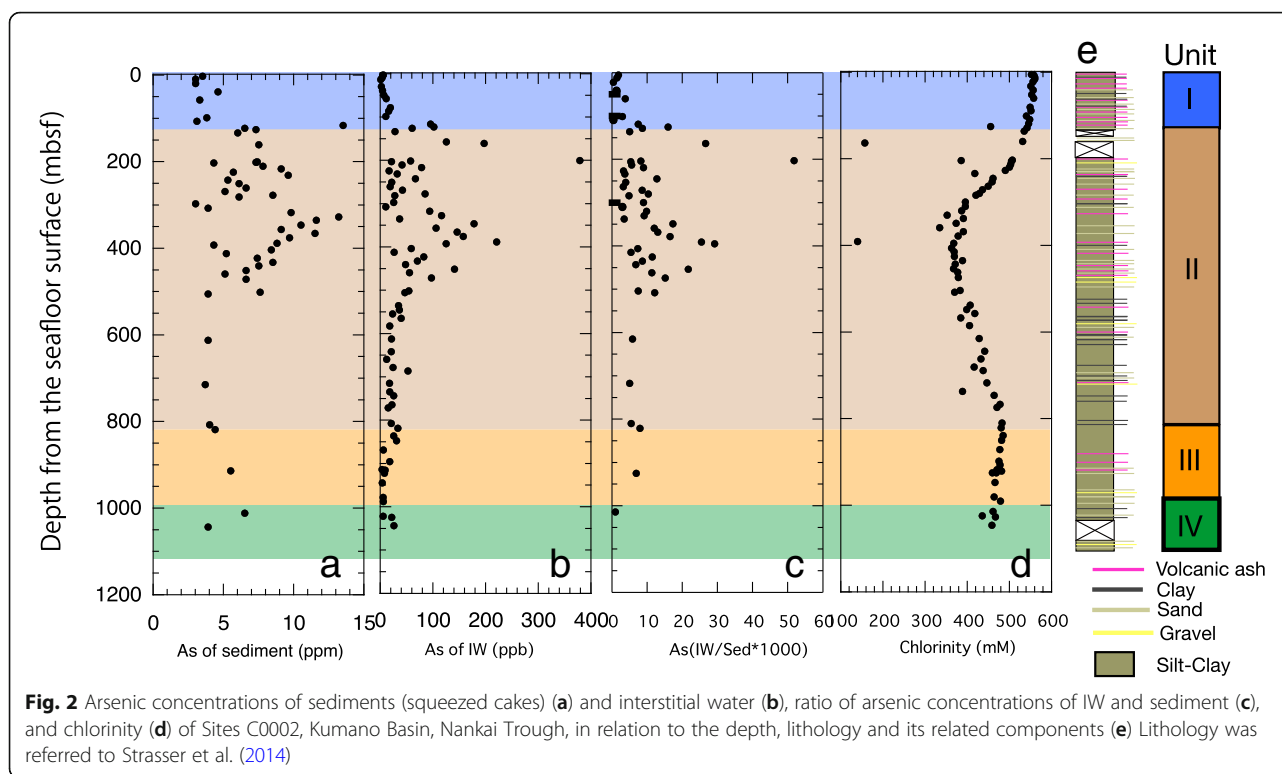


Fig. 1 Location of study sites (Sites C0002, C0021, and C0022, Kumano Basin, Nankai Trough) (a) and geological profile of the area (b) (Strasser et al. 2014)

Total As concentration

One gram of powdered sediment was fused with NaCO₃ at 900 °C until the silicates were completely melted, and then the residue was dissolved in 0.05 M HNO₃. IW was diluted with 0.05 M HNO₃ to make a 1/300 solution. Total As concentrations in the sample solutions were

quantified by inductively coupled plasma-mass spectrometry (ICP-MS; SPQ9700, Hitachi), with H₂ gas used to prevent the formation of ArCl⁺. Commercially distributed standard As solution (FUJIFILM Wako Pure Chemical Corp.) was used for the calibration. Accuracy of the results was checked by using rock standard samples



(JSd-1, As 2.42 ppm; JSd-2, 38.6 ppm; and JSI-1, 14.9 ppm) from AIST (National Institute of Advanced Industrial Science and Technology), which were prepared in a similar manner to the studied samples. The analytical error was $\pm 8\%$ at maximum.

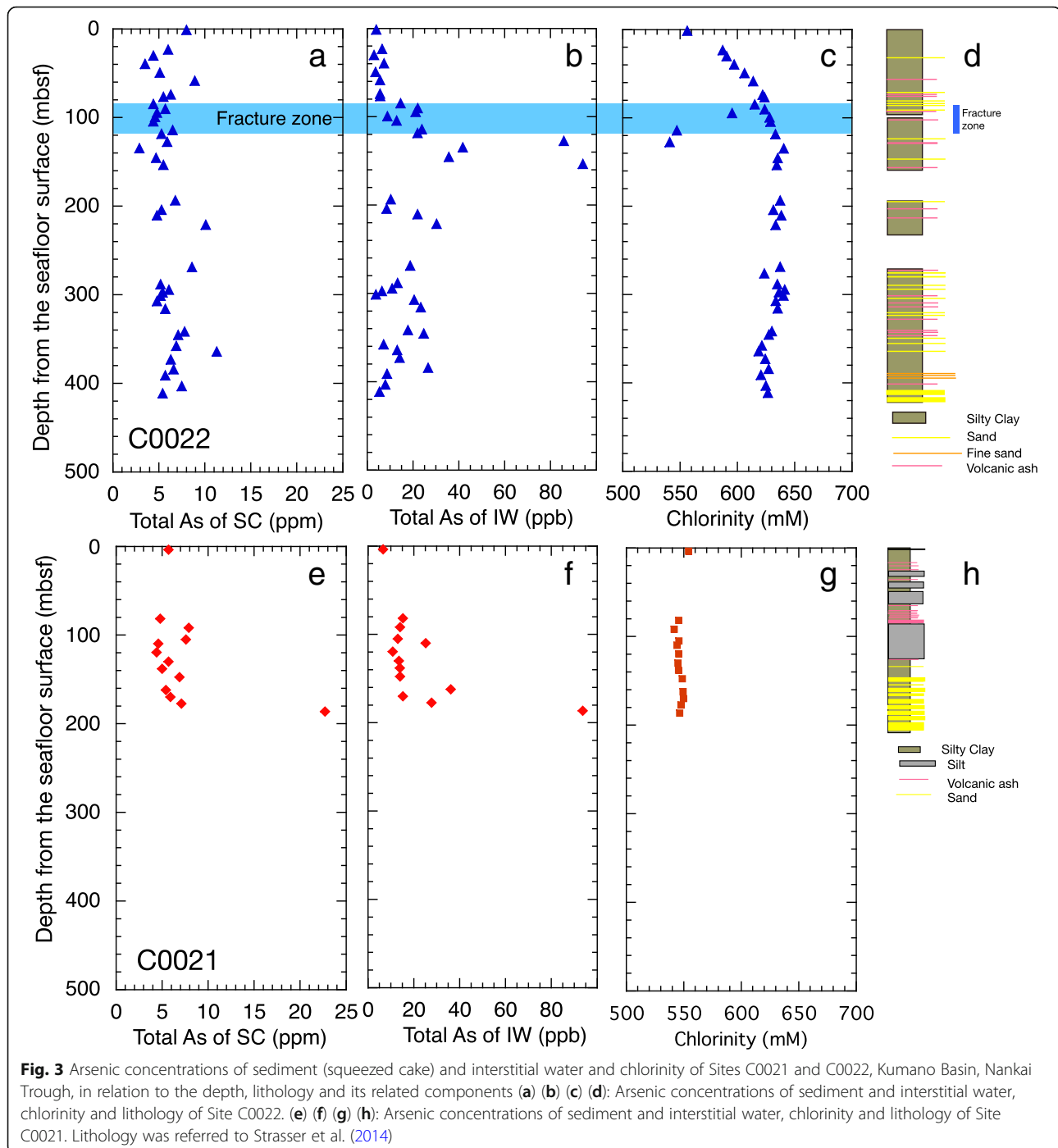
Sequential chemical extraction of As

The BCR sequential chemical extraction method (Rauret et al. 1999) was used to separate chemical phases of As in sediment. This method cannot accurately specify the As host phases, but As behaviors associated with changes in the environmental redox condition can be roughly evaluated. As phases were extracted in five steps. In step 1, 1 g of sediment powder was put in a PTFE centrifuge tube, which was shaken with 20 ml 0.22 M acetic acid (pH adjusted to 5 with HNO_3) for 16 h at room temperature. Then, the mixture was centrifuged at 10,000 rpm for 10 min to extract acid-soluble phases, namely, components weakly adsorbed onto detrital materials or contained in carbonates into the supernatant fluid. In step 2, the residual sediment was washed with ultra-pure water; then, 20 ml 0.5 M hydroxylammonium chloride (NH_2OHCl , pH adjusted to 2 with HNO_3) was added and the mixture was shaken for 16 h at room temperature to extract As fixed in reducible phases, mainly, Fe-oxyhydroxides and Mn-oxides. In step 3, the residue from the previous step was heated with 20 ml 0.1 M sodium pyrophosphate solution for 2 h

and then shaken with 5 M ammonium acetate ($\text{CH}_3\text{COONH}_4$, pH 2) for 16 h. This reagent cannot completely decompose sulfide minerals, so the most probable phase dissolved at this step is organic matter. Then, the mixture of residue and solution was centrifuged to separate. In step 4, the residue from step 3 was shaken with a mixture of concentrated nitric and perchloric acid for 16 h, then gently heated for 24 h, and centrifuged. Most insoluble phases, silicates, and sulfides were decomposed at this step. In step 5, the residue from the previous step was decomposed by alkaline fusion to decompose minerals resistant to the reagents used in steps 1–4. The As extracted at each step was quantified by ICP-MS as described in the previous section.

As species in sediments

Water-soluble As compounds in SC from Sites C0002 and C0022 were extracted by the method of Ellwood and Maher (2003). The sediment sample was mixed with a solution of 0.1 M hydroxylammonium chloride and 0.5 M phosphoric acid in a PTFE centrifuge tube and shaken at 25 °C for 1 h. The hydroxylammonium chloride solution is reductant and can decompose amorphous and weakly crystallized Fe-oxyhydroxides (e.g., ferrihydrite and goethite) and Mn-oxides, and the phosphoric acid helps to preserve As^{III} and As^{V} species, especially in solutions containing high amounts of Fe and Mn (Ellwood and Maher 2003). Frozen sediment was used for this analysis, because dried samples may become



oxidized, changing the chemical form of the As. After the reaction, the solid phase was separated by centrifugation (1880×g for 10 min) and removed by filtration through a PTFE membrane filter (0.45 μm mesh). The obtained solution was analyzed by HPLC–ICP–MS at the National Institute for Environmental Studies (8800 ICP–QQQ, Agilent Technologies, Inc., USA) to determine the concentrations of each separated As phase. Eight As compounds (commercially distributed by

FUJIFILM Wako Pure Chemical Corp.), As(III), As(V), methylarsonic acid (MMA), dimethylarsinic acid (DMA), arsenobetaine (AsB), trimethylarsine oxide (TMO), tetramethylarsonium salt (TMAO), and arsenocholine (AsC), were separated in a GL–Science InertSil AS column (4.6 i.d. × 250 mm long), using an eluent composed of 10 mM butane-1-sulfonic acid sodium salt, 4 mM malonic acid, 4 mM tetramethylammonium hydroxide, and 0.05% methanol. The flow rate was 1.0 ml/min at 40 °C.

Results

Bulk As concentration

The bulk As concentrations in SC from Hole C0002 ranged from 3 to 14 ppm (average 6.4 ppm) (Table 1, Fig. 2a), which is within the range of reported concentration in seafloor surface sediments surrounding the Japanese islands; for example, an average concentration of As of 5.5 ppm (range, 0–14 ppm, except one sample with 23.3 ppm) has been reported for 95 surface sediment samples from Kumano-nada (the sea area around the study area) (AIST 2018).

The highest As concentration was measured in SC from 116 mbsf, at the bottom of Unit I (13.5 ppm), but the As concentration range in SC from other parts of Unit I was low (3–5 ppm). In the upper half of Unit II, between 110 and 500 mbsf (referred to as Unit II-1 hereafter), the As concentration was > 5 ppm, and a maximum concentration of 13.2 ppm was observed at 320 mbsf. Arsenic concentrations of SC from below 600 mbsf in Hole C0002 were mostly < 5 ppm, similar to those of SC from Unit I. The bulk As concentration in sediments from below 2000 mbsf was also mostly < 6 ppm, while it increased in the deeper part and the maximum concentration was up to 11 ppm (Table 1). Although only bulk As concentrations were obtained from the deepest sediments, we inferred that As behavior did not largely change below ~ 500 mbsf in Hole C0002.

The total dissolved As concentration of IW from Hole C0002 ranged from 0.9 to 379 ppb (average 50 ppb). The total As concentration was low in the Unit I sediments and in the sediments from below 500 mbsf (Units II-2 and III), whereas it was high in the Unit II-1 sediments (Fig. 2b). The relationship between the SC concentration and the IW concentration varied with depth (Fig. 2c); for example, As peaks in IW were observed at 200 and 400 mbsf, whereas sediment peaks were observed at 116 and < 350 mbsf. The low As concentrations in SC from Unit I (excepting three samples from the bottom of the unit) and from below 500 mbsf did not change with depth. Owing to the insoluble host phases of the As and the physico-chemical conditions of the ambient IW, As in these depth intervals would not be easily mobilized.

At Site C0022, the drilled hole penetrated the fracture zone of a splay fault at around 100 mbsf (Fig. 3). The chlorinity of the IW increased with depth from 550 mM, that of ambient seawater, to 600 mM in the fracture zone, reflecting the upwelling of deep-seated water, in which dissolved salts had been concentrated via hydration reactions, along the fault (Strasser et al. 2014). The total As concentration in SC and IW ranged from 3 to 11 ppm and 4 to 94 ppb, respectively. The total concentration in SC did not change with depth, whereas that in IW increased below 100 mbsf and reached a peak at 110–130 mbsf, below the fracture zone.

Total As concentrations of SC and IW from Hole C0021 were from 4 to 7 ppm and from 7 to 36 ppb, respectively, except the deepest sample (22.7 ppm and 94 ppb), and did not change substantially with depth (Fig. 3). This site is located on the forearc slope, and the cored sediments consist of landslide deposits. The chlorinity is stable with depth and the same as that of seawater, probably because the sediment and IW were homogenized during relocation by the landslide. Thus, except in the deepest samples (from 180 mbsf), the As concentrations in the sediment (4–9 ppm) and IW (5–20 ppb) can be regarded as averaged shallow sediment values.

Host phases of As in the sediments

Total As recovery by sequential extraction is reported as a percentage relative to the bulk As concentration (Table 2). In the sequential chemical extraction of As phases from sediments of Hole C0002, the total recovery of As ranged from 65.4 to 146.7% (average and 1 σ : 104 \pm 20%, Table 2 and Fig. 4). Among the totally extracted As, recovery in steps 1, 2, and 3, which extracted the mobile As phases in association with changing redox and pH conditions of coexisting solution, ranged from 10 to 70%; As recovery in steps 2 and 3 averaged 21% and 19%, respectively. Further, As extracted in step 3, of which main host phase is organic matter, seemed to increase as the total As concentration of the sample increased ($r=0.72$); this result implies that biogenic As was responsible for the high accumulation rate of As in this sediment column. The high concentrations of As extracted from Unit II in step 2, which extracted As associated with Fe-oxyhydroxides/Mn oxides, imply that oxidation of Fe-minerals occurred in this unit.

As species in sediments separated by HPLC

The mixture of hydroxyl-ammonium chloride solution and phosphoric acid leaches inorganic and organic phases adsorbed onto Fe-hydroxides and other particles. The leached phases may correspond partly to As extracted by steps 1, 2, and 3 of the sequential extraction procedure. Only sediments from Unit II of C0002 (recovery 30–100%) and from C0022 (recovery 20 to 80%) were analyzed by this procedure. These recoveries are generally high compared with the summed As concentrations sequentially extracted by steps 1, 2, and 3 (Table 3), probably because the analytical error of the leaching procedure is slightly higher than that for the total As concentration measurement.

Even considering the large analytical error, it is notable that the most abundant leached As phase was arsenate (As^V) (Fig. 5); this result indicates that the As was mostly adsorbed onto or fixed in Fe-oxyhydroxides in the

Table 1 Total arsenic concentration of squeezed cake and interstitial water of sediments from the Sites C0002, C0021 and C0022 at Nankai Trough

Sample name	Depth (mbsf)	As concentration	
		Squeezed cake (ppm)	Interstitial water (ppb)
C0002D-1H-2	2	3.5	5.1
C0002D-1H-5	4		4.8
C0002D-2H-3	9	3.0	3.1
C0002D-2H-7	13		0.9
C0002D-3H-4	19	3.0	
C0002D-4H-4	29		2.0
C0002D-5H-4	38	4.6	4.0
C0002D-6H-5	49		6.4
C0002D-7H-4	57	3.3	11.1
C0002D-9H-5	78		18.8
C0002D-10H-4	86		15.5
C0002D-11H-5	98	3.8	10.0
C0002D-12H-5	106	3.1	
C0002D-13H-5	116	13.5	95.4
C0002D-14H-3	122	6.5	101.5
C0002D-14H-5	125	7.3	60.1
C0002D-15X-5	133	6.0	27.8
C0002D-16H-6	157		125.1
C0002D-17X-4	160	7.5	196.8
C0002D-18H-1	200	7.4	378.7
C0002D-18H-2	201	7.3	57.5
C0002K-1H-3	202	4.3	21.2
C0002K-3T-5	210	7.8	41.0
C0002K-4T-2	216	9.1	77.9
C0002K-5T-6	224	5.7	16.3
C0002K-6T-3	231	9.6	31.9
C0002K-7X-5	242	5.3	66.3
C0002K-8X-2	250	6.1	21.4
C0002K-9X-3	260	6.6	18.6
C0002K-10X-2	268	5.1	41.6
C0002K-11X-2	277	8.5	84.8
C0002L-1X-4	281	6.1	27.4
C0002L-3X-2	297	3.0	25.3
C0002L-4X-2	307	3.9	10.3
C0002L-5X-3	317	9.8	93.6
C0002L-6X-4	327	13.2	115.9
C0002L-7X-2	335	11.6	36.4
C0002L-8X-4	346	10.5	177.8
C0002L-9X-5	356	9.1	105.7
C0002L-10X-3	365	11.5	145.5
C0002L-11X-4	375	9.7	157.2

Table 1 Total arsenic concentration of squeezed cake and interstitial water of sediments from the Sites C0002, C0021 and C0022 at Nankai Trough (Continued)

Sample name	Depth (mbsf)	As concentration	
		Squeezed cake (ppm)	Interstitial water (ppb)
C0002L-12X-7	388	8.8	220.4
C0002P 2R-1	2173	2.5	
C0002P 2R-2	2175	2.5	
C0002P 2R-3	2176	3.6	
C0002P 2R-4	2177	8.7	
C0002P 3R-1	2182	6.6	
C0002P 4R-1	2192	4.9	
C0002P 4R-4	2196	4.3	
C0002P 4R-6	2199	5.4	
C0002P 4R-7	2203	2.5	
C0002P 4R-8	2212	6.4	
C0002P 4R-9	2213	11.6	
C0002P 4R-10	2214	8.0	
C0002P 4R-11	2217	8.9	
C0021B-1H-4	3.7	5.7	6.6
C0021B-2H-3	81.6	4.8	15.2
C0021B-3H-4	91.7	7.9	14.0
C0021B-4H-6	104.9	7.6	13.0
C0021B-5H-2	109.9	4.6	25.2
C0021B-6H-3	119.5	4.4	10.8
C0021B-7H-4	129.9	5.7	13.5
C0021B-8H-2	138.0	5.0	13.9
C0021B-9H-2	147.5	6.9	14.0
C0021B-10H-8	162.1	5.4	36.1
C0021B-12H-2	170.0	5.9	15.3
C0021B-13T-3	177.4	7.1	27.8
C0021B-14T-2	186.4	22.7	93.7
C0022B-1H-2	1.2	8.0	4.0
C0022B-2H-5	23.4	6.0	6.5
C0022B-3H-2	30.3	4.4	3.0
C0022B-4H-2	39.5	3.5	7.4
C0022B-5H-2	49.3	5.1	3.7
C0022B-6H-2	58.6	8.9	5.6
C0002L-13X-1	392	4.3	124.8
C0002L-14X-3	403	8.4	58.4
C0002L-15X-4	412	5.2	25.8
C0002L-16X-3	422	7.4	82.3
C0002L-17X-4	432	8.5	70.0
C0002L-18X-3	440	7.5	47.8
C0002L-19X-3	451	6.6	140.6
C0002L-20X-2	459	5.1	55.3

Table 1 Total arsenic concentration of squeezed cake and interstitial water of sediments from the Sites C0002, C0021 and C0022 at Nankai Trough (*Continued*)

Sample name	Depth (mbsf)	As concentration	
		Squeezed cake (ppm)	Interstitial water (ppb)
C0002L-21X-4	471	6.6	96.9
C0002L-24X-5	501	7.6	54.2
C0002B-4R-2	505	3.9	46.2
C0002B-8R-2	535		34.4
C0002B-9R-3	545		35.9
C0002B-10R-2	554		23.1
C0002B-11R-3	564		39.2
C0002B-13R-2	582		17.8
C0002B-16R-3	612	3.9	21.1
C0002B-19R-3	641		20.7
C0002B-21R-3	659		12.1
C0002B-23R-3	678		23.9
C0002B-24R-2	686		52.3
C0002B-27R-2	714	3.7	17.3
C0002B-29R-2	734		17.8
C0002B-30R-2	743		25.4
C0002B-32R-5	764		21.7
C0002B-33R-2	771		14.8
C0002B-37R-2	807	4.0	20.4
C0002B-38R-3	818	4.4	33.3
C0002B-40R-2	836		25.3
C0002B-41R-3	847		30.5
C0002B-43R-5	868		5.5
C0002B-46R-4	895		17.6
C0002B-48R-5	915		8.8
C0002B-49R-3	922		7.7
C0002B-51R-5	944		3.5
C0002B-55R-2	978		5.1
C0002B-56R-2	987		5.5
C0002B-59R-2	1011	6.5	
C0002B-61R-3	1021		5.3
C0002B-62R-2	1024		21.3
C0002B-64R-2	1043	3.9	25.5
C0002J-3R-3	913.6	5.5	3.3
C0022B-7H-7	74.0	6.3	5.6
C0022B-8H-1	76.5	5.5	5.7
C0022B-9T-2	84.8	4.4	14.6
C0022B-10T-2	90.3	5.7	22.1
C0022B-11T-1	94.5	4.8	21.2
C0022B-12T-1	99.5	4.6	8.8

Table 1 Total arsenic concentration of squeezed cake and interstitial water of sediments from the Sites C0002, C0021 and C0022 at Nankai Trough (*Continued*)

Sample name	Depth (mbsf)	As concentration	
		Squeezed cake (ppm)	Interstitial water (ppb)
C0022B-13T-1	104.5	4.4	12.8
C0022B-14X-4	114.1	6.5	23.9
C0022B-15X-3	118.5	5.3	22.0
C0022B-16X-4	127.5	5.9	85.8
C0022B-17X-2	134.8	2.9	41.7
C0022B-18X-4	145.6	4.7	35.6
C0022B-19X-2	153.4	5.5	94.1
C0022B-20X-4	193.6	6.8	10.3
C0022B-21X-6	204.3	5.3	8.5
C0022B-22X-1	210.5	4.8	22.0
C0022B-23X-4	221.2	10.1	30.3
C0022B-24X-3	268.7	8.6	18.8
C0022B-26X-3	288.3	5.2	13.3
C0022B-27X-4	294.3	6.1	10.9
C0022B-28X-3	297.4	5.4	6.4
C0022B-29X-2	301.3	5.2	3.8
C0022B-30X-3	307.3	4.8	20.5
C0022B-31X-2	315.9	5.7	23.4
C0022B-33X-7	341.7	7.8	17.8
C0022B-34X-3	345.4	7.1	24.7
C0022B-35X-5	357.8	6.9	7.2
C0022B-36X-3	364.2	11.3	13.1
C0022B-37X-2	373.1	6.3	14.2
C0022B-38X-3	384.3	6.6	26.6
C0022B-39X-2	391.0	5.7	8.7
C0022B-40X-3	403.2	7.5	7.9
C0022B-41X-2	411.4	5.4	5.4

sediments. In addition, chromatogram peaks indicating small amounts of MMA and AsB and two unidentified As compounds were detected. Chromatogram peaks for the identifiable compounds were confirmed by co-injection of standards of As-compounds. The presence of above organoarsenicals indicates that As in the sediment column had a biological source.

Discussion

We examined the factors controlling As behavior in deep-sea sediments mainly on the basis of the analytical results for the cored sediments from Hole C0002. Vertical profiles of As and other chemical components in IW from the sediment column at Site C0002 are shown in Fig. 6 (Moore et al. 2013). As described above, chlorinity

Table 2 Arsenic concentrations of sequentially extracted fractions of sediments from Site C0002 at Nankai Trough

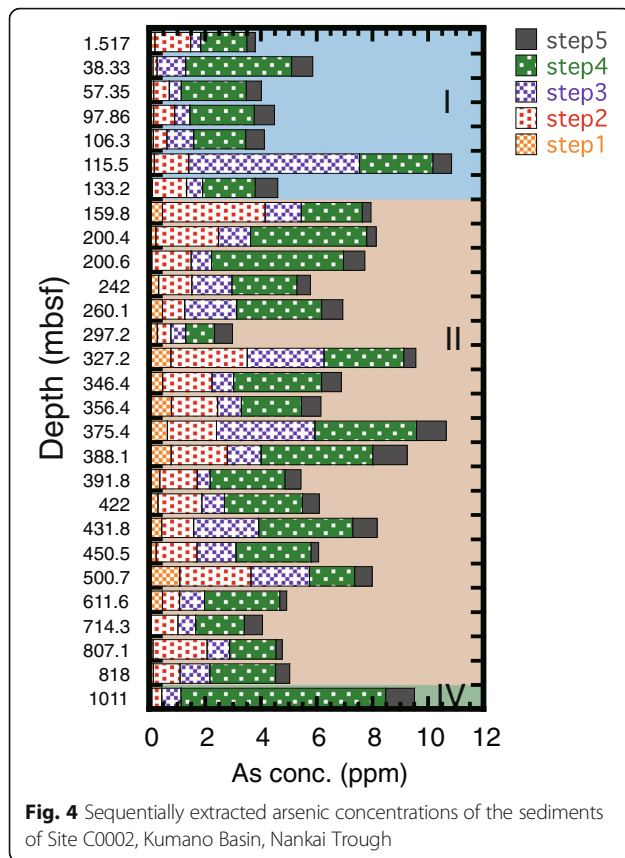
Sample name	Depth (mbsf)	Total As(ppm)	As concentration (ppm)					Recovery (%)	
			Step 1	Step 2	Step 3	Step 4	Step 5		Total
C0002D 1H-2	2	3.5	0.18	1.27	0.36	1.67	0.29	3.76	107.3
C0002D 5H-4	38	4.6	0.10	0.15	1.03	3.80	0.76	5.84	127.7
C0002D 7H-4	57	3.3	0.13	0.57	0.42	2.34	0.54	3.99	121.9
C0002D 11H-5	98	3.8	0.12	0.76	0.54	2.31	0.72	4.46	116.2
C0002D 12H-5	106	3.1	0.11	0.49	0.97	1.86	0.67	4.10	132.7
C0002D 13H-5	116	13.5	0.15	1.24	6.12	2.64	0.66	10.81	80.2
C0002D 15X-5	133	6.0	0.08	1.23	0.57	1.88	0.82	4.58	76.7
C0002D 17X-4	160	7.5	0.44	3.69	1.30	2.19	0.31	7.92	105.8
C0002D 18H-1	200	7.4	0.21	2.24	1.14	4.18	0.33	8.11	110.2
C0002D 18H-2	201	7.3	0.06	1.41	0.73	4.73	0.77	7.71	104.9
C0002K 7X-5	242	5.3	0.30	1.19	1.44	2.33	0.49	5.75	107.6
C0002K 9X-3	260	6.6	0.44	0.80	1.86	3.05	0.75	6.91	105.4
C0002L 3X-2	297	3.0	0.25	0.49	0.53	1.04	0.64	2.95	100.0
C0002L 6X-4	327	13.2	0.75	2.74	2.76	2.86	0.43	9.53	72.3
C0002L 8X-4	346	10.5	0.45	1.78	0.77	3.17	0.70	6.86	65.4
C0002L 9X-5	356	9.1	0.76	1.66	0.85	2.15	0.70	6.13	67.7
C0002L 11X-4	375	9.7	0.62	1.76	3.52	3.65	1.06	10.62	109.2
C0002L 12X-7	388	8.8	0.76	2.01	1.21	4.01	1.22	9.22	104.8
C0002L 13X-1	392	4.3	0.35	1.34	0.46	2.69	0.58	5.42	125.2
C0002L 16X-3	422	7.4	0.28	1.57	0.81	2.79	0.61	6.07	81.6
C0002L 17X-4	432	8.5	0.41	1.15	2.33	3.38	0.87	8.14	96.1
C0002L 19X-3	451	6.6	0.21	1.46	1.40	2.70	0.27	6.05	91.8
C0002L 24X-5	501	7.6	1.06	2.56	2.10	1.63	0.63	7.97	104.9
C0002B 16R-3	612	3.9	0.44	0.61	0.89	2.71	0.24	4.90	125.5
C0002B 27R-2	714	3.7	0.03	0.96	0.64	1.74	0.65	4.03	108.6
C0002L 37R-2	807	4.0	0.10	1.95	0.81	1.67	0.22	4.74	117.5
C0002B 38R-3	818	4.4	0.11	0.96	1.07	2.36	0.51	5.01	114.9
C0002B 59R-2	1011	6.5	0.07	0.35	0.69	7.35	1.03	9.48	146.7

decreases linearly in Units I, III, and IV, whereas in Unit II, freshwater derived from the dissociation of methane hydrate diluted the IW, lowering the chlorinity of that unit. Here, we first discuss differences in the vertical variation of chemical components likely controlled by in situ microbial activity; later, we discuss sources of the IW.

In Unit I, reduction of SO_4^{2-} occurred just beneath the seafloor, leading to a low SO_4^{2-} concentration there. The Fe concentration is also low in Unit I, probably owing to the precipitation of FeS_2 (pyrite), because framboidal pyrite was observed throughout the sediment column (Strasser et al. 2014). Br^- , PO_4^{3-} , and NH_4^+ increase with depth in Unit I; these results can be plausibly attributed to the decomposition of organic matter. Peak concentrations of these three components were observed in the uppermost part of Unit II; below that, their concentrations decreased with depth down to 400 mbsf.

The SO_4^{2-} concentrations of Unit II are higher than those of the Unit I, in which SO_4^{2-} reduction occurs just beneath the ocean bottom surface (Fig. 6). The similar decrease (3–6 mbsf) and increase (> 400 mbsf) of SO_4^{2-} concentrations were observed in the deep-sea sediments at IODP Sites 1173 and 1174 at Nankai Trough, about 100 km SW from this study site. In those sediment columns, high SO_4^{2-} was supplied from diffusive flux of sulfate from the oceanic basement into the overlying sediments (e.g., Shipboard Scientific Party 2001a, b; Heuer et al. 2017). It would not be the case for the sediment column studied here, since the upward migration of deep fluid was limited (Toki et al. 2017). However, the SO_4^{2-} would be derived diffusive flux of seawater and/or deep-sourced fluid (BG, described in the next paragraph).

We examined variations of IW chemistry in relation to the end-member composition of the IW (Fig. 7). Toki et al.



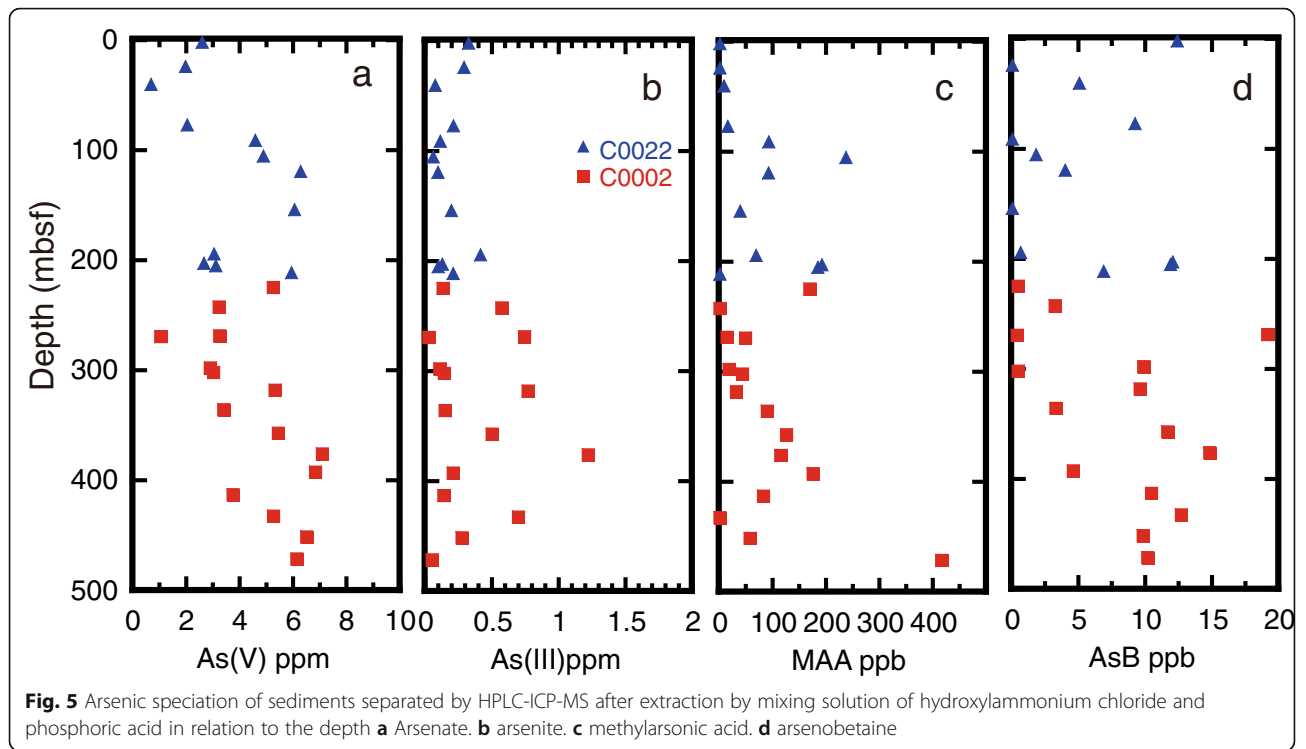
(2017) inferred that IW at Site C0002 is a mixture of three end members: SW (seawater); MH, freshwater derived from the dissociation of methane hydrate; and BG, defined as a deep-sourced fluid probably formed by ultrafiltration during burial diagenesis of IW in the old accretionary prism (Fig. 7a). SW, MH, and BG are characterized by chlorinity values of 550, 140, and 460 mM, respectively, and $\delta^{18}\text{O}$ values of 0‰, +1‰, and -2.5‰, respectively. These three end members are typically found at the seafloor surface, around the methane hydrate concentration peak at about 400 mbsf, and below 1000 mbsf, respectively. Toki et al. (2017) suggested that the IW initially formed by the mixing of SW and BG via slow advection and was later modified by the addition of MH to the mixture. Most IW from Units I, III, and IV represents a mixture of SW and BG, whereas IW from Unit II is a mixture of MH with pre-existing SW–BG mixture. Concentrations of dissolved components associated with microbial activity and redox conditions are not just a simple function of the mixing ratios of the three end members. Figure 7 shows relationships among chemical components plausibly vary associated with As. Some components show contrasting distributions in four separate depth intervals: for example, Br^- is enriched but the Cl^- concentration is unchanged from that of SW in Unit I, both Cl^- and Br^- are depleted in MH, and Cl^- is depleted with no change in the Br^- concentration in BG

Table 3 Arsenic concentrations of soluble fractions extracted by hydroxylammonium chloride and phosphoric acid solution

Sample name	Depth (mbsf)	Concentration			
		As(V) (ppm)	As(III)/As(III) (ppm)	MAA (ppm)	AsB (ppm)
C0002K-1H-3	202	2.64	0.13	0.19	0.01
C0002K-5 T-6	224	5.23	0.13	0.17	0.00
C0002K-7X-5	242	3.20	0.57	0.00	0.00
C0002K-10X-2	268	3.22	0.74	0.01	0.02
C0002L-3X-2	297	2.87	0.10	0.02	0.01
C0002L-5X-3	317	5.29	0.77	0.03	0.01
C0002L-7X-2	335	3.37	0.14	0.09	0.00
C0002L-9X-5	356	5.42	0.50	0.12	0.01
C0002L-11X-4	375	7.07	1.22	0.11	0.01
C0002L-13X-1	392	6.81	0.21	0.17	0.00
C0002L-15X-4	412	3.73	0.14	0.08	0.01
C0002L-17X-4	432	5.25	0.69	0.00	0.01
C0002L-19X-3	451	6.49	0.27	0.06	0.01
C0002L-21X-4	471	6.11	0.05	0.41	0.01
C0022B-1H-2	1	2.56	0.32	0.00	0.01
C0022B-2H-5	23	1.95	0.29	0.00	0.00
C0022B-4H-2	39	0.66	0.07	0.01	0.01
C0022B-8H-1	77	2.01	0.21	0.01	0.01
C0022B-10 T-2	90	4.56	0.11	0.09	0.00
C0022B-13X-1	105	4.87	0.06	0.24	0.00
C0022B-15X-3	118	6.26	0.09	0.09	0.00
C0022B-19X-2	153	6.02	0.19	0.04	0.00
C0022B-20X-4	194	3.01	0.41	0.07	0.00
C0022B-21X-6	204	3.08	0.09	0.18	0.01
C0022B-22X-1	210	5.91	0.21	0.00	0.01
C0022B-24X-3	269	1.01	0.02	0.05	0.00
C0022B-29X-2	301	3.00	0.14	0.04	0.00

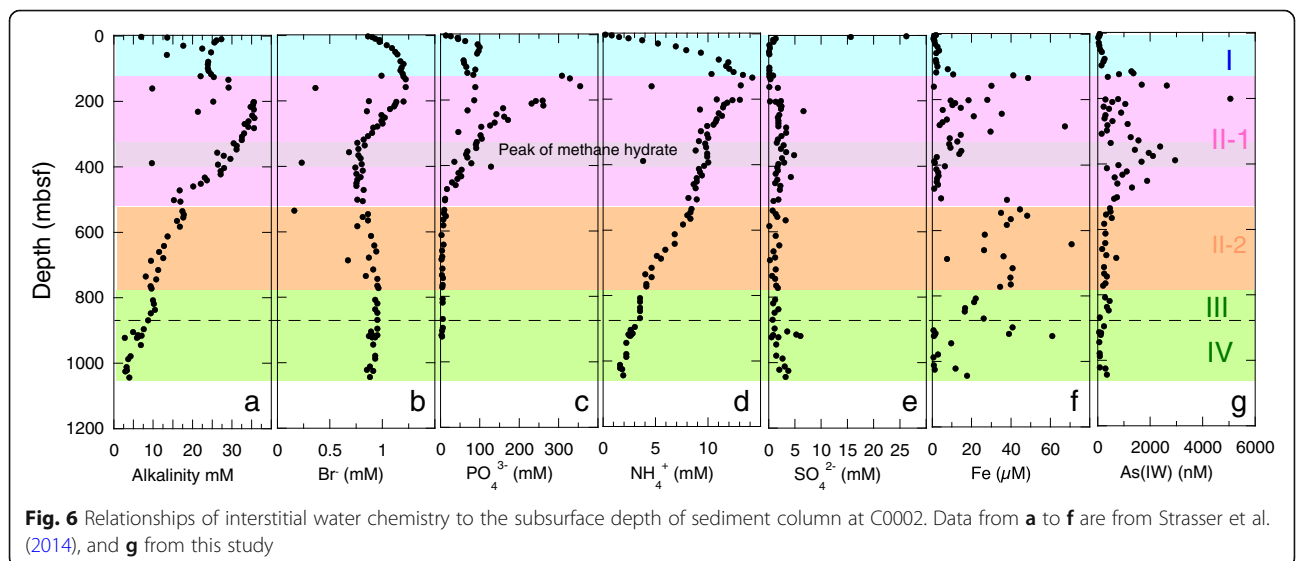
(in Units III and IV) (Fig. 7b). Br^- , PO_4^{3-} , and NH_4^+ show weakly positive correlations in Unit I, whereas those components show strongly positive correlations in Unit II-1. IW from Units III and IV is characterized by low PO_4^{3-} without changes in Br^- and NH_4^+ concentrations (Fig. 7c, d). In Unit II-1, the Fe concentration seems to increase with the PO_4^{3-} concentration (Fig. 7e). These features suggest that the IW geochemistry reflects the degree of biological degradation, and that microbial activity was most active in Unit II-1.

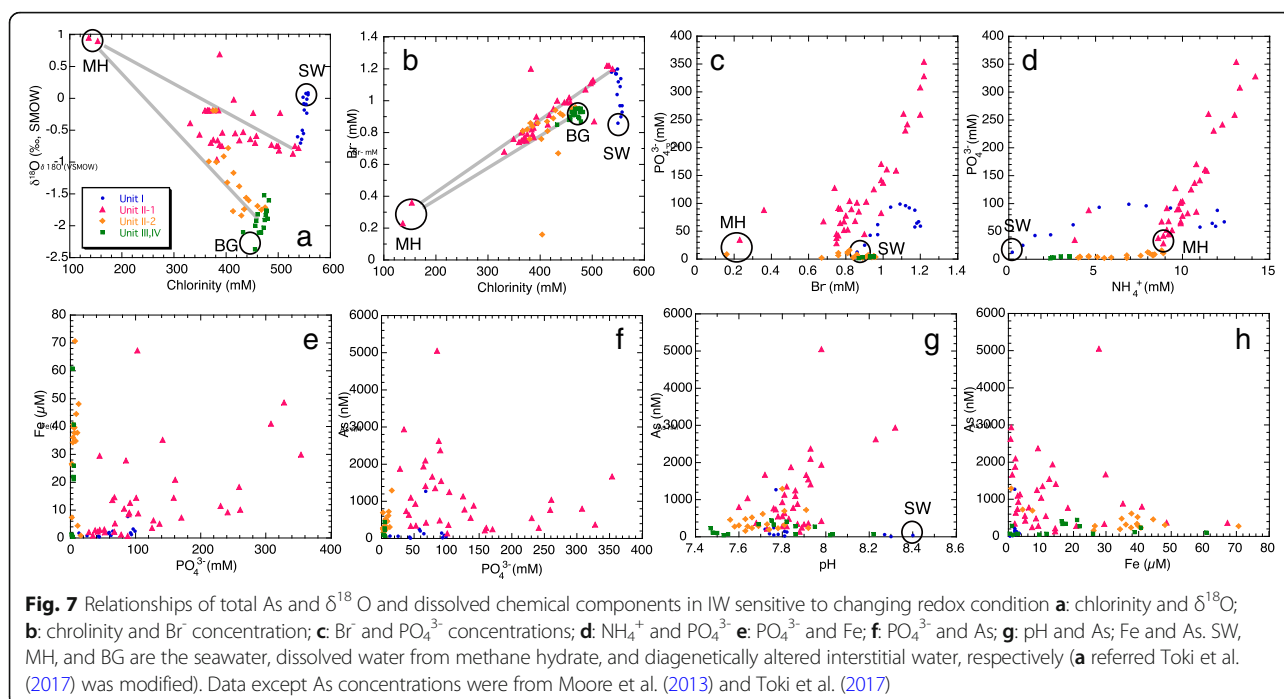
The Br^- concentration (Fig. 6b), but not the Cl^- concentration, of IW increased with depth in Unit I, probably because Br was released from sediments by the decomposition of Br-containing organic matter derived from algae and marine animals, some of which



concentrate Br in various, mostly toxic, compounds such as bromoperoxidases (Hewson and Hager 1980), bromoform, and dibromoacetic acid (DBA) (e.g., Paul et al. 2006). Further, alkyl bromide compounds (Ma et al. 2010) have been extracted from algae, and 2,4-dibromophenol is produced by animal activity in coastal sediments (King 1988). Dehalogenation bacteria were recovered from the sediment column of Hole C0002 down to 150 mbsf, and Futagami et al. (2013) observed dehalogenation (bromide release) of 2,4,6-tribromophenol in an incubation

experiment conducted with sediment from 4.7 mbsf. The freshwater derived from the dissociation of methane hydrate is not only low in Cl^- but also in Br^- (Fig. 7a). The BG end member is slightly depleted in Cl^- but not in Br^- compared with SW. IW from Unit II was a mixture of MH, SW, and BG. The Br^- concentration increased with increasing PO_4^{3-} in Units I and II-1. High Br^- and PO_4^{3-} concentrations are probably attributable to the decomposition of algae, and the relationship between them showed different trends between Units I and II-1. Moreover, the





relationship between NH_4^+ and PO_4^{3-} in IW showed different trends even more clearly between Units I and II-1. These differences between Units I and II-1 suggest that the sources of Br^- , PO_4^{3-} , and NH_4^+ differed between these Units (Fig. 7c, d). IW was depleted PO_4^{3-} in Unit III and IV, and the relationship to Br^- and NH_4^+ can be explained by the mixing of BG and MH.

The high bulk As concentrations in both sediment and IW in Unit II-1 (Fig. 2), along with the high Br^- , PO_4^{3-} , and NH_4^+ concentrations of IW, imply that these components had similar sources, i.e., marine biology especially such as algae. In Unit II-1, the As concentration increased with increasing pH (Fig. 7g) but not in relation to either PO_4^{3-} or Fe (Fig. 7f, h). From the combined results of sequential extraction and leaching analyses, we can infer that a considerable amount of As^{V} was associated with Fe-oxyhydroxides and that the As concentration of IW was largely controlled by the pH. The adsorption–desorption affinity of As onto Fe-oxyhydroxides is mainly controlled by the solution pH; adsorption of arsenate (As^{V}) occurs at pH 5–6, whereas desorption becomes dominant at higher pH (e.g., Pearce and Moore 1982; Bowell et al. 1994; Dixit and Hering 2003).

MMA, one of the simplest organoarsenicals, is derived from the decomposition of arsenosugars contained in phytoplankton and algae (Edmonds et al. 1997; Morita and Shibata 1990). AsB (arsenobetaine), the simplest protein containing As, is derived from marine animals (e.g., Francesconi and Edmonds 1996). Decomposition rates of organic As in sediments are high: Takeuchi et al. (2005) observed that in surface sediments from a coastal

area, which were plausibly more oxic than the deep-sea sediments studied here, organic As was largely decomposed within approximately 60 years. The ages of the sediments from 200 to 500 mbsf in Hole C0002K and C0002L, corresponding to Unit II-1 in this study, were constrained from 1.04 to 1.34 Ma by biostratigraphy and magnetostratigraphy conducted during Expedition 315 (Strasser et al. 2014; Expedition 315 Scientists 2009). MMA can form in situ by microbial methylation (Reimer and Thompson 1988) in conjunction with methane formation. Sulfate-reducing and nitrogen-fixing bacteria were detected with methanogen, which mostly uses CO_2 and H_2 for producing CH_4 , from the sediments down to 193.29 mbsf at IODP Site 1173, located in the Nankai Trough and about 100 km SW of our study site (Newberry et al. 2004). In the same sediment column down to 194 mbsf, epsilon-proteobacterial clones, of which species used a diverse spectrum of electron acceptors, such as O_2 in low concentrations, NO_3^- , S^0 , and $\text{S}_2\text{O}_3^{2-}$, were also detected, and it was notable that these clones could also respire with Fe(III) and arsenate (Kormas et al. 2003). The similar microbial assemblage would be expected in the Unit II-1 of our studied column, of which IW contained SO_4^{2-} . AsB, an organic As compound that is synthesized and degraded in biotransformation cycles, is ubiquitous in marine, terrestrial, and deep-sea hydrothermal systems (Hoffmann et al. 2018). In light of the results reported by Hoffmann et al. (2018), we can infer that the AsB in the deep-sea sediments studied here was also a product of in situ microbial activity. Thus, the detection of organic As compounds suggests that considerable amounts of

mobile As in the studied sediment column may have been derived in relation to microbial activity via both degradation and synthesis of organic As compounds in the sediment column.

Conclusions

Arsenic is actively released into IW at depths of methane hydrate layer of deep-sea sediments of the Nankai Trough, offshore Japan. The release of As accompanies the degradation of organic matter and following change of redox condition to control the adsorption/desorption affinity of As onto the Fe-oxyhydroxides. The sources of the As in the sediment column are not clear at present. However, a considerable amount of mobile As must be derived from marine organisms. It is notable that As mobilization in deep-sea sediments is associated with microbial activity in deep-sea sediments where methane hydrate appears.

Acknowledgements

The authors sampled the studied sediments and IW in collaboration with the crews and onboard scientists of Expeditions 338 and 348. The stored samples taken during Expedition 315 were provided by the Kochi Core Center, which is directed by Dr. Lalan Gupta. T. Shimonaka and K. Okazaki supported for conducting shore-based laboratory analyses. The comments from Dr. T. Kakegawa and two anonymous reviewers were helpful to improve the manuscript. We thank to all of them. This study was financially supported by post-cruise IODP studies to HM, SF and EE, and KAKENHI (No. 17K18810).

Funding

Samples were collected on Drilling Vessel “Chikyu” under IODP program during Expeditions 338 and 348. Post cruise research fund from JAMSTEC for HM, SF and EE and KAKENHI (No. 17K18810) were used for As analyses.

Availability of data and materials

All data newly obtained from this study is in the manuscript and data sharing is not applicable.

Authors' contributions

HM carried out the sample collection and pretreatments on Exp. 338, helped in the analysis of water-soluble As, wrote the manuscript, and drew the figures. HY helped in the analyses of As of interstitial water and sediments. SF helped in the sample collection and pretreatments on Exp. 348, analysis of water-soluble As with HY, and discussion. TT helped in the sample collection and pretreatments on Exp. 338, and discussion. EE contributed to the sample collection and pretreatments on Exp. 348. All authors read and approved the final manuscript.

Competing interests

The authors declare that they have no competing interests.

Publisher's Note

Springer Nature remains neutral with regard to jurisdictional claims in published maps and institutional affiliations.

Author details

¹Department of Biology and Geosciences, Graduate School of Science, Osaka City University, 3-3-138 Sugimoto, Sumiyoshi-ku, Osaka 558-8585, Japan.

²Present Address: Marine Environment Section, Center for Regional Environmental Research, National Institute for Environmental Studies, 16-2 Onogawa, Tsukuba, Ibaraki 305-8506, Japan. ³Department of Chemistry, Biology and Marine Science, Faculty of Science, University of the Ryukyus, 1 Senbaru, Nishihara, Okinawa 903-0123, Japan.

Received: 30 April 2018 Accepted: 27 January 2019

Published online: 21 March 2019

References

- AIST (2018) Geochemical map of sea and land of Japan. <https://gbank.gsj.jp/geochemmap/ocean/data/ganyuryo/ocean-noudo.csv>. (18 Apr 2018)
- Andreae MO (1979) Arsenic speciation in seawater and interstitial waters: the influence of biological-chemical interactions on the chemistry of a trace element. *Limnol Ocean* 24:440–452
- Ashi J, Lallemand S, Masago H, the Expedition 315 Scientists (2008) NanTroSEIZE stage 1A: NanTroSEIZE megasplay riser pilot. IODP Prel Rept 315. <https://doi.org/10.2204/iodp.pr.315.2008>
- Bowell RJ, Morley NH, Din VK (1994) Arsenic speciation in porewaters, Ashanti mine, Ghana. *Appl Geochem* 9:9–14
- Dixit S, Hering JG (2003) Comparison of arsenic(V) and arsenic(III) sorption onto Iron oxide minerals: implications for arsenic mobility. *Environ Sci Technol* 37: 4182–4189. <https://doi.org/10.1021/es030309t>
- Duncan EG, Hafer WA, Foster SD (2015) Contribution of arsenic species in unicellular algae to the cycling of arsenic in marine environment. *Environ Sci Technol* 49:33–50
- Edmonds JS, Francesconi KA, Cannon JR, Raston CL, Skelton BW, White AH (1977) Isolation, crystal structure and synthesis of arsenobetaine, the essential constituent of the western rock lobster *Panulirus longipes cygnus* George. *Tetrahedron Lett* 18:1543–1546
- Edmonds JS, Francesconi KA, Rippingale RJ, Morita M (1997) Arsenic transformations in short marine food chains studied by HPLC-ICP MS. *App Organometal Chem* 11:281–287
- Ellwood MJ, Maher WA (2003) Measurement of arsenic species in marine sediments by high-performance liquid chromatography-inductively coupled plasma mass spectrometry. *Anal Chim Acta* 477:279–291
- Expedition 315 Scientists (2009) Expedition 315 site C0001. In: Kinoshita M, Tobin H, Ashi J, Kimura G, Lallemand S, Sreaton EJ, Curewitz D, Masago H, Moe KT, the Expedition 314/315/316 Scientists (eds) Proc. IODP, 314/315/316. Integrated Ocean Drilling Program Management International, Inc, Washington, DC. <https://doi.org/10.2204/iodp.proc.314315316.123.2009>
- Expedition 348 Scientists and Scientific Participants (2014) NanTroSEIZE stage 3: NanTroSEIZE plate boundary deep riser 3. IODP Prel Rept 348. <https://doi.org/10.2204/iodp.pr.348.2014>
- Francesconi KA, Edmonds JS (1996) Arsenic and marine organisms. *Adv Inorg Chem* 44:147–189
- Futagami T, Morono Y, Terada T, Kaksanen AH, Inagaki F (2013) Distribution of dehalogenation activity in subseafloor sediments of the Nankai Trough subduction zone. *Phil Trans Royal Soc B* 368. <https://doi.org/10.1098/rstb.2012.0249>
- Handley KM, Lloyd JR (2013) Biogeochemical. implications of the ubiquitous colonization of marine habitats and redox gradients by *Marinobacter* species. *Front Microbiol* 4:1–10.
- Heuer VB, Inagaki F, Morono Y, Kubo Y, Maeda L, Expedition 370 Scientists (2017) Expedition 370 preliminary report: temperature limit of the deep biosphere off Muroto. International Ocean Discovery Program. <https://doi.org/10.14379/iodp.pr.370.2017>
- Hewson WC, Hager LP (1980) Bromoperoxidases and halogenated lipids in marine algae 1. *J Phycol*. <https://doi.org/10.1111/j.1529-8817.1980.tb03043.x>
- Hoffmann T, Warmbold B, Smits SHJ, Tschapek B, Ronzheimer S, Bashir A, Chen C, Rolbetzki A, Pittelkow M, Jebbar M, Seubert A, Schmitt L, Bremer E (2018) Arsenobetaine: an ecophysiological important organoarsenical confers cytoprotection against osmotic stress and growth temperature extremes. *Environ Microbiol* 20:305–323
- King GM (1988) Dehalogenation in marine sediments containing natural sources of halophenols. *Appl Environ Microbiol* 54:3079–3085
- Kormas KA, Smith DC, Edgcomb V, Teske A (2003) Molecular analysis of deep subsurface microbial communities in Nankai Trough sediments (ODP leg 190, site 1176). *FEMS Microbiol Ecol* 45:115–125
- Ma JM, Cai LL, Zhang BJ, Hu LW, Li XY, Wang JJ (2010) Acute toxicity and effects of 1-alkyl-3-methylimidazolium bromide ionic liquids on green algae. *Ecotoxicol Environ Safety* 73:1465–1469
- Manheim FT (1966) A hydraulic squeezer for obtaining interstitial waters from consolidated and unconsolidated sediments. *Geol Surv Prof Pap (U.S.)* 550-C: 256–261
- Masuda H (2018) Arsenic cycling in the Earth's crust and hydrosphere: interaction between naturally occurring arsenic and human activities. *Prog Earth Planet Sci* 5:68. <https://doi.org/10.1186/s40645-018-0224-3>

- Moore G, Kanagawa K, Strasser M, Dugan B, Maeda L, Toczko S, the Expedition 338 Scientists (2013) NanTroSEIZE stage 3: NanTroSEIZE plate boundary deep riser 2. In: IODP Prelim Rep. Integrated Ocean Drilling Program Management International, Inc
- Moore GF, Park JO, Bangs NL, Gulick SP, Tobin HJ, Nakamura Y, Saito S, Tsuji T, Yoro T, Tanaka H, Uraki S, Kido Y, Sanada Y, Kuramoto S, Taira A. (2009) Structural and seismic stratigraphic framework of the NanTro-SEIZE State 1 transect: Kumano 3D seismic survey. In: Kinoshita, M., Tobin, H., Ashi, J., Kimura, G., Lallement, S., Sreaton, E.J., Curewitz, D., Masago, H., Moe, K.T., Scientists, E. (Eds.), Proceedings of the Integrated Ocean Drilling Program. Integrated Ocean Drilling Program Management International, Inc, 46
- Morita M, Shibata Y (1990) Chemical form of arsenic in marine macroalgae. *Appl Organomet Chem* 4:181–190
- Neff JM (2002) Chapter 3 — Arsenic in the ocean, Bioaccumulation in Marine Organisms. Elsevier, Oxford, pp. 57–78.
- Newberry CJ, Webster G, Cragg BA, Parkes RJ, Weightman AJ, Fry JC (2004) Diversity of prokaryotes and methanogenesis in deep subsurface sediments from the Nankai Trough, Ocean Drilling Program leg 190. *Environ Microbiol* 6:274–287
- Paul NA, de Nys R, Steinberg PC (2006) Chemical defence against bacteria in the red alga *Asparagopsis armata*: linking structure with function. *Mar Ecol Prog Ser* 306:87–101
- Pearce ML, Moore CB (1982) Adsorption of arsenite and arsenate on amorphous iron hydroxides. *Water Res* 16:1247–1253
- Raab A, Fecher P, Feldmann J (2005) Determination of arsenic in algae—results of an interlaboratory trial: determination of arsenic species in the water-soluble fraction. *Microchim Acta* 151:153–166
- Rauret G, López-Sánchez JF, Sahuquillo A, Rubio R, Davidson C, Ure A, Quevauviller P (1999) Improvement of the BCR three step sequential extraction procedure prior to the certification of new sediment and soil reference materials. *J Environ Monit* 1:57–61
- Reimer KJ, Thompson JA (1988) Arsenic speciation in marine interstitial water. The occurrence of organoarsenicals. *Biogeochem* 6:211–237
- Sanders JG (1979) The concentration and speciation of arsenic in marine macroalgae. *Estuar Coast Mar Sci* 9:95–99
- Shipboard Scientific Party (2001a) Site 1173. In: Moore GF, Taira A, Klaus A et al (eds) Proceedings of the Ocean Drilling Program, Initial Reports, 190. Ocean Drilling Program, College Station, pp 1–147. <https://doi.org/10.2973/odp.proc.ir.190.104.2001>
- Shipboard Scientific Party (2001b) Site 1174. In: Moore GF, Taira A, Klaus A et al (eds) Proceedings of the Ocean Drilling Program, Initial Reports, 190. Ocean Drilling Program, College Station, pp 1–149. <https://doi.org/10.2973/odp.proc.ir.190.105.2001>
- Strasser M, Dugan B, Kanagawa K, Moore GF, Toczko S, Maeda L, the Expedition 338 Scientists (2014) Proc. IODP, 338. Integrated Ocean Drilling Program, Yokohama. <https://doi.org/10.2204/iodp.proc.338.2014>
- Takeuchi M, Terada A, Nanba K, Kanai Y, Owaki M, Yoshida T, Kuroiwa T, Nirei H, Komai T (2005) Distribution and fate of biologically formed organoarsenicals in coastal marine sediment. *Appl Organometal Chem* 19:945–951
- Toki T, Kinoshita M, Morita S, Masuda H, Rashid H, Yoshinishi H, Nakano T, Noguchi T (2017) The vertical chloride ion profile at the IODP site C0002, Kumano Basin, off coast of Japan. *Tectonophysics* 710-711:88–96

Submit your manuscript to a SpringerOpen[®] journal and benefit from:

- Convenient online submission
- Rigorous peer review
- Open access: articles freely available online
- High visibility within the field
- Retaining the copyright to your article

Submit your next manuscript at ► [springeropen.com](https://www.springeropen.com)